

ON THE HOMOGENEOUS MODEL OF WIND-DRIVEN OCEAN CIRCULATION*

B. DESJARDINS^{†‡} AND E. GRENIER^{†§}

Abstract. In this paper, we derive rigorously a classical simplified model of ocean circulation, namely the so-called homogeneous model of wind-driven ocean circulation [J. Pedlosky, *Geophysical Fluid Dynamics*, Springer–Verlag, 1979] and two of its possible boundary-layer behaviors, namely Munk layers and Stommel layers.

Key words. boundary layers, Navier–Stokes equation, oceanography

AMS subject classifications. 76U05

PII. S0036139997324261

Introduction. This paper is the fourth of a series dedicated to the derivation of some basic and classical equations of meteorology, following the classical physics source book of J. Pedlosky [16]. The series began with the analysis of inertial waves ([7] corresponding to [16, Chapter 3]), and continued with the study of Ekman layers [10], [16, Chapter 4] and the derivation of quasi-geostrophic potential vorticity equations [3, Chapter 6], [16]. Here we present a mathematical justification of a classical equation of meteorology, which describes the motion of the ocean in the presence of wind (as studied in [16, Chapter 5]), namely the homogeneous wind-driven model of the ocean. The substantive “homogeneous” refers to the fact that the limit flow is two-dimensional, and “wind-driven” refers to the external force applied on the free surface of the ocean. In spite of its simplicity, this model catches some of the main features of ocean motion (see the end of [16, Chapter 5]), like the importance of Ekman layers and the Ekman pumping term created by a very small (turbulent) viscosity, the role of bottom topography, and the role of the wind. Moreover it is a starting point for further analyses, like the western intensification of boundary currents [16] and the study of the Sverdrup relation and Munk and Stommel boundary layers.

Topographical effects have been extensively studied by Levermore, Oliver, and Titi in [13] for the so-called great lake equations, where variations of the ocean depth are of the order of the depth itself (and not small with respect to the averaged depth as in the present case), which is possible since the Rossby number does not go to zero in their model. (In fact there is no Coriolis force and no wind and, therefore, no boundary layers.)

Let (u_1, u_2) be the two-dimensional velocity of the fluid and p its pressure. We want to derive the following system in a domain $\Omega_2 \in \mathbb{R}^2$:

$$(0.1) \quad u_1 = -\partial_y p, \quad u_2 = \partial_x p, \quad \zeta = \text{curl}(u_1, u_2) = \Delta p,$$

*Received by the editors July 14, 1997; accepted for publication (in revised form) October 5, 1998; published electronically November 10, 1999.

<http://www.siam.org/journals/siap/60-1/32426.html>

[†]Département de Mathématiques et d’Informatique, Ecole Normale Supérieure, 45 rue d’Ulm, 75005 Paris, France (egrenier@upma.ens-lyon.fr, benoit.desjardins@na-net.ornl.gov).

[‡]CEREMADE, Université Paris Dauphine, Place de Lattre de Tassigny, 75775 Paris Cedex 16, France.

[§]Laboratoire d’Analyse Numérique, C.N.R.S. U.R.A. 189, Université Paris 6, Place Jussieu, 75252 Paris Cedex 05, France.

$$(0.2) \quad \left(\partial_t + u_1 \partial_x + u_2 \partial_y \right) \left(\zeta + \beta y + \eta_B \right) = \beta \operatorname{curl} \tau + \frac{1}{Re} \Delta \zeta - \frac{r_0}{2} \zeta,$$

$$(0.3) \quad u_1 = u_2 = 0 \quad \text{on} \quad \partial\Omega_2,$$

where η_B is a given function that describes the bottom topography of the ocean and r_0 and β are given scalars characterizing the Ekman pumping and the β -plane approximation.

Let us make a short analysis of these equations:

- $d/dt = \partial_t + u_1 \partial_x + u_2 \partial_y$ is the transport operator by the two-dimensionnal limit flow,
- ζ is the vorticity and $-r_0 \zeta / 2$ is the Ekman pumping term,
- $\beta dy/dt = \beta u_2$ is created by the variation of the Coriolis force with respect to the latitude (under the β -plane approximation),
- $d\eta_B/dt = u_1 \partial_x \eta_B + u_2 \partial_y \eta_B$ is the vorticity created by the nonuniform bottom,
- $\beta \operatorname{curl} \tau$ is the vorticity generated by the wind, and
- $\Delta \zeta / Re$ is the usual viscous term.

In the first section we derive formally these equations, following [16] (we also refer to [1] for a short formal nearby derivation), and in the second section we justify them by constructing approximate solutions and making energy estimates. As the derivation is somewhat technical, we postpone the statement of the main result till the second part. In the third and fourth sections we investigate the limit $\beta \rightarrow +\infty$ of (0.1), (0.2), (0.3), and the associated Munk and Stommel boundary layers, which appear along western boundaries. These boundary layers are used in meteorology to explain the general features of the mean oceanic circulation as created by the wind. These layers differ from Ekman layers because the viscosity remains constant and does not go to zero, whereas the velocity blows up and goes to infinity as the small parameter goes to zero. The last section is devoted to numerical simulations, which illustrate the theoretical analysis of this paper.

1. Formal derivation of the equations.

1.1. Navier–Stokes equations in a rotating frame. We start with the Navier–Stokes equations in a rotating frame, with viscous dissipation represented by \mathcal{F}_0 :

$$(1.1) \quad \partial_t u + (u \cdot \nabla) u + 2\vec{\Omega} \times u = -\frac{\nabla p}{\rho} + \vec{g} + \frac{1}{\rho} \mathcal{F}_0 u, \quad \nabla \cdot u = 0,$$

where $u(t, x, y, z)$ is the three-dimensional velocity of the fluid, \vec{g} the gravity force, $\vec{\Omega}$ a constant vector (direction of the rotation, $2\vec{\Omega} \times u$ being the Coriolis force), ρ the constant density, and \mathcal{F}_0 the turbulent viscosity (to be described later).

Let R_0 denote the radius of the earth and set $z = r - R_0$. We consider the fluid motion in a bounded domain Ω_3 defined in spherical coordinates (r, ϕ, θ) by

$$\Omega_3 = \{(z, \phi, \theta) \mid (\phi, \theta) \in \Omega_2, \quad h_B(x, y) \leq z \leq 0\},$$

where the upper surface of the ocean is assumed to be flat at $z = 0$, $h_B(x, y)$ describes the topography of the bottom of the ocean, and Ω_2 is a two-dimensional open set. Notice that deviations from a constant gravity field do not contribute to the limit system, so that we drop the r dependence of \vec{g} in order to simplify the notations.

As boundary conditions, we enforce

$$(1.2) \quad u = 0 \quad \text{on} \quad z = h_B(x, y), \quad u = 0 \quad \text{on} \quad (\phi, \theta) \in \partial\Omega_2,$$

and

$$(1.3) \quad \sigma_{\phi,r} = \gamma\tau^{(x)}, \quad \sigma_{\theta,r} = \gamma\tau^{(y)}, \quad \text{and} \quad u_3 = 0 \quad \text{on} \quad z = 0,$$

where $(\tau^{(x)}, \tau^{(y)})$ is a given stress tensor describing the wind on the surface of the ocean, γ is a normalized parameter that will be described later, and $\sigma_{\phi,r} = e_\phi \cdot (\sigma \cdot e_r)$, $\sigma_{\theta,r} = e_\theta \cdot (\sigma \cdot e_r)$ are two components of the stress tensor σ of the fluid. We assume that there exists $A_0 > 0$ such that

$$(1.4) \quad \sigma_{\phi,r} = 2A_0 d_{\phi,r} \quad \text{and} \quad \sigma_{\theta,r} = 2A_0 d_{\theta,r},$$

where $d_{\phi,r}$ and $d_{\theta,r}$ are, respectively, the (ϕ, r) and the (θ, r) components of the deformation tensor of the velocity field u . These two components are expressed in spherical coordinates as

$$(1.5) \quad d_{\phi,r} = \frac{1}{2} \left(\frac{1}{r \cos \theta} \partial_\phi u_3 + \partial_r u_1 - \frac{1}{r} u_1 \right), \quad d_{\theta,r} = \frac{1}{2} \left(\frac{1}{r} \partial_\theta u_3 + \partial_r u_2 - \frac{1}{r} u_2 \right).$$

Notice that (1.3) is a rigid lid approximation, and we assume that the upper surface of the ocean remains at $z = 0$. This is a drastic but standard simplification, since it is actually a free surface and a moving interface between air and water, which has its own self-consistent motion. The justification of (1.3) starting from a free surface is open (see [13] for works in this direction in the context of the great lake equation). From a meteorological point of view, however, the simplification does not appear to be so dramatic, since in any case the free surface is so turbulent with waves and even foam that only a modelization is tractable and meaningful. Condition (1.3) is a simple modelization that already catches most of the physical phenomena (see [5] for other formulas).

1.2. Scaled Cartesian-like coordinates. Let L and D be the typical horizontal and vertical lengths of Ω_3 and U be the typical velocity, and define Cartesian-like coordinates by

$$(1.6) \quad x = \frac{\phi R_0 \cos \theta_0}{L}, \quad y = \frac{(\theta - \theta_0) R_0}{L}, \quad \text{and} \quad z = \frac{r - R_0}{D},$$

θ_0 being a typical latitude far enough from the poles and the equator. We also rescale \vec{u} , t , p , and h_B as follows:

$$(u_1, u_2) = U(u'_1, u'_2), \quad u_3 = \frac{UD}{L} u'_3, \quad t = \frac{L}{U} t',$$

$$p = -\rho g z + 2 \sin \theta_0 \Omega \rho U L p', \quad h_B = D h'_B, \quad r_\star = \frac{R_0}{L},$$

and rescale τ . (We will not keep track of the rescaling of τ .) Rewriting (1.1) in the new variables and new unknown functions and dropping the primes gives

$$(1.7) \quad \frac{du_1}{dt} + \frac{u_1(\delta u_3 - u_2 \tan \theta)}{r_\star + \delta z} + \frac{\delta u_3 \cos \theta - u_2 \sin \theta}{\varepsilon \sin \theta_0} = -\frac{\cos \theta_0 \partial_x p}{\varepsilon \cos \theta (1 + \delta z / r_\star)} + \frac{1}{\rho} \mathcal{F} u_1,$$

$$(1.8) \quad \frac{du_2}{dt} + \frac{\delta u_3 u_2}{r_* + \delta z} + \frac{u_1^2}{r_* + \delta z} \tan \theta + \frac{\sin \theta}{\varepsilon \sin \theta_0} u_1 = -\frac{\partial_y p}{\varepsilon(1 + \delta z/r_*)} + \frac{1}{\rho} \mathcal{F} u_2,$$

$$(1.9) \quad \frac{du_3}{dt} - \frac{u_1^2 + u_2^2}{\delta(r_* + \delta z)} - \frac{u_1 \cos \theta}{\delta \varepsilon \sin \theta_0} = -\frac{\partial_z p}{\delta^2 \varepsilon} + \frac{1}{\rho} \mathcal{F} u_3,$$

$$(1.10) \quad \left(\frac{1}{1 + \delta z/r_*} \right) \left(\frac{\cos \theta_0}{\cos \theta} \partial_x u_1 + \frac{1}{\cos \theta} \partial_y (u_2 \cos \theta) \right) + \frac{2u_3}{r_* + \delta z} + \partial_z u_3 = 0$$

with

$$(1.11) \quad u_1 = u_2 = u_3 = 0 \quad \text{when} \quad z = h_B \quad \text{or} \quad (\phi, \psi) \in \partial \Omega_2,$$

$$(1.12) \quad \partial_z u_1 + \frac{\delta^2 \cos \theta_0}{1 + \delta z/r_*} \partial_x u_3 - \frac{\delta}{1 + \delta z/r_*} u_1 = \frac{D\gamma}{A_0 U} \tau^{(x)},$$

$$(1.13) \quad \partial_z u_2 + \frac{\delta^2}{1 + \delta z/r_*} \partial_y u_3 - \frac{\delta}{1 + \delta z/r_*} u_2 = \frac{D\gamma}{A_0 U} \tau^{(y)} \quad \text{at} \quad z = 0,$$

where

$$\theta = \theta_0 + \frac{y}{r_*}, \quad \frac{d}{dt} = \partial_t + \frac{\cos \theta_0}{\cos \theta (1 + \delta z/r_*)} (u_1 \partial_x + u_2 \partial_y) + u_3 \partial_z,$$

and where the Rossby number ε and the aspect ratio δ are defined by

$$(1.14) \quad \varepsilon = \frac{U}{2\Omega \sin \theta_0 L} \quad \text{and} \quad \delta = \frac{D}{L}.$$

1.3. Ordering of the parameters. We refer to [5] and in particular to [16, Chapter 4] for a physical discussion of these equations and their asymptotic behavior. It is usual to take an anisotropic viscosity

$$(1.15) \quad \mathcal{F} = -A_H \Delta_{x,y} - A_V \partial_{zz}^2 \quad \text{or} \quad \frac{1}{\rho} \mathcal{F} = -\nu_H \Delta_{x,y} - \nu_V \partial_{zz}^2$$

after the above scaling operations. Here, ν_H and ν_V are defined by

$$(1.16) \quad \nu_H = \frac{A_H}{\rho U L} \quad \text{and} \quad \nu_V = \frac{L A_V}{\rho U D^2}.$$

We will study the following asymptotic behavior (among other possibilities, it seems to be the most “physical” one; see [16]):

$$(1.17) \quad \varepsilon \rightarrow 0, \quad \nu_H \sim 1, \quad \nu_V \sim \varepsilon, \quad \delta \sim \varepsilon, \quad L/R_0 \sim \varepsilon.$$

Let us give some geophysical values of ν_V , ν_H , δ , ε , L/R_0 . For the mesoscale or synoptic eddies that have been observed in the western Atlantic [16], $U \sim 5$ cm/s, $L \sim 100$ km, $2\Omega \sin \theta_0 \sim 10^{-4}$ s $^{-1}$, $D \sim 4$ km. This leads to $\varepsilon \sim 5 \times 10^{-3}$, $\delta \sim 2 \times 10^{-2}$, $L/R_0 \sim 2 \times 10^{-2}$. Moreover, if we take $A_H \sim 10^7$ cm 2 /s and $A_V \sim 10$ cm 2 /s (which are possible values [16, Chapter 4]), $\nu_H \sim 2$ and $\nu_V \sim 10^{-3}$. Notice that $A_H \neq A_V$ is natural in a geophysical framework and comes from a modelization of turbulence [16, Chapter 4].

Moreover, to have topographic effects of order one we will take

$$(1.18) \quad h_B(x, y) = -1 + \varepsilon \eta_B(x, y),$$

where η_B is a given smooth function. Notice that the bottom has variations of very small amplitude, but this already leads to $O(1)$ terms in the limit equations. Therefore (1.18) is the right scaling when the Rossby number and the viscosities go to zero. It is also the scaling usually used in meteorology. When the variations are larger, the limit motion is very constrained, and Taylor–Proudman columns appear (see [6]). In [13], Levermore, Oliver, and Titi are able to deal with large variations of h_B because they have no large Coriolis force and no small viscosity.

Let us point out that this paper concentrates on the case $\nu_H \sim 1$ in order to avoid the study of boundary layers near $(\phi, \theta) \in \partial\Omega_2$. These boundary layers are usually studied in a second step on the limit system deduced from (1.7), (1.8), (1.9) by the limit $\varepsilon \rightarrow 0$.

1.4. Formal limit. Assume that u_1 , u_2 , u_3 , and p converge respectively to u_1^0 , u_2^0 , u_3^0 , and p^0 . Then using (1.7), (1.8), (1.9) at order ε^{-1} or $\varepsilon^{-1}\delta^{-2}$, we get, using (1.17),

$$(1.19) \quad u_1^0 = -\partial_y p^0, \quad u_2^0 = \partial_x p^0, \quad \partial_z p^0 = 0.$$

Hence p^0 , u_1^0 , and u_2^0 are independent on x and y . Moreover, $\partial_x u_1^0 + \partial_y u_2^0 = 0$, which leads to $u_3^0 = 0$. Equations (1.19) are called geophysical constraints and define the “geostrophic wind.”

To get an evolution equation on p^0 , we have to study the next order of the expansion and assume that $u_1 = u_1^0 + \varepsilon u_1^1$ and similarly for u_2 , u_3 , and p . Taking the two-dimensional curl of (1.7), (1.8) and setting $\zeta^0 = \partial_x u_2^0 - \partial_y u_1^0$, we get, using (1.17),

$$\partial_t \zeta^0 + u_1^0 \partial_x \zeta^0 + u_2^0 \partial_y \zeta^0 + \beta v^0 - \nu_H \Delta_{x,y} \zeta^0 + \partial_x u_1^1 + \partial_y u_2^1 = 0,$$

where

$$(1.20) \quad \beta = \lim_{\varepsilon \rightarrow 0} \frac{r_\star \cos \theta_0}{\varepsilon \sin \theta_0}.$$

Using (1.10), we get

$$(1.21) \quad \partial_t \zeta^0 + u_1^0 \partial_x \zeta^0 + u_2^0 \partial_y \zeta^0 - \nu_H \Delta_{x,y} \zeta^0 + \beta v^0 = -\partial_z u_3^1.$$

Since ζ_0 , u_1^0 , and u_2^0 are independent on z , we can integrate (1.21) to get

$$\partial_t \zeta^0 + u_1^0 \partial_x \zeta^0 + u_2^0 \partial_y \zeta^0 - \nu_H \Delta_{x,y} \zeta^0 + \beta v^0 = -u_3^1(t, x, y, 0) + u_3^1(t, x, y, -1 + \varepsilon \eta_B).$$

As usual in geostrophic flows, the evolution of ζ^0 is determined by the deviation from equilibrium state at order ε [16, 3]. It remains to evaluate u_3^1 at $z = 0$ and $z = -1$. For this we need a detailed analysis of the boundary layers (called Ekman layers), which is performed in the next section.

1.5. Bottom Ekman layer. The boundary layer equations are obtained by looking for solutions u of the form

$$u(t, x, y, z) = u^0(t, x, y, z) + u^b(t, x, y, \xi), \quad \text{where} \quad \xi = \frac{z + 1 - \varepsilon \eta_B}{\sqrt{2\varepsilon\nu_V}},$$

and

$$u^b(t, x, y, 0) = -u^0(t, x, y).$$

Putting this Ansatz in (1.7), (1.8), (1.9) and keeping the predominant terms, we obtain the following [16]:

$$(1.22) \quad \frac{u_2^b}{\varepsilon} + \frac{\partial_{\xi\xi}^2 u_1^b}{2\varepsilon} = \frac{1}{\varepsilon} \partial_x p^b, \quad \frac{u_1^b}{\varepsilon} - \frac{\partial_{\xi\xi}^2 u_2^b}{2\varepsilon} = -\frac{1}{\varepsilon} \partial_y p^b, \quad 0 = \frac{1}{\delta^2 \varepsilon \sqrt{\varepsilon \nu_V}} \partial_\xi p^b.$$

Hence, using the third equation of (1.22), as is usual in fluid boundary layers, the pressure p^b does not vary in the boundary layer and is given by the pressure inside the domain. Hence $p^b = 0$. This leads to the study of

$$(1.23) \quad u_2^b = -\frac{1}{2} \partial_{\xi\xi}^2 u_1^b \quad \text{and} \quad u_1^b = \frac{1}{2} \partial_{\xi\xi}^2 u_2^b$$

(see [16, 3, 10]). The solution of (1.23) is determined by

$$(1.24) \quad u_1^b(t, x, y, \xi) = -(u_1^0(t, x, y) \cos \xi + u_2^0(t, x, y) \sin \xi) e^{-\xi},$$

$$(1.25) \quad u_2^b(t, x, y, \xi) = (u_1^0(t, x, y) \sin \xi - u_2^0(t, x, y) \cos \xi) e^{-\xi},$$

exactly as the Ekman layers for incompressible rotating fluids. Using the incompressibility condition, we in particular deduce

$$(1.26) \quad u_3^b(t, x, y, \xi) = -\varepsilon(u_1^b \partial_x \eta_B + u_2^b \partial_y \eta_B) - \frac{\sqrt{\varepsilon \nu_V}}{2} \zeta^0(t, x, y) (\sin \xi + \cos \xi) e^{-\xi}$$

and

$$(1.27) \quad u_3^1(t, x, y, -\delta + \varepsilon \eta_B) = -\lim_{\xi \rightarrow +\infty} \varepsilon^{-1} u_3^b(t, x, y, \xi) = u^0 \cdot \nabla_{x,y} \eta_B + \frac{r_0}{2} \zeta^0$$

if $\nu_V = r_0^2 \varepsilon$. The first term in (1.27) describes the effect of the topography and the second term is called the Ekman pumping term.

1.6. Top Ekman layer. The derivation is similar except we use the limit boundary conditions

$$(1.28) \quad \partial_z u_1 = \frac{D\gamma}{A_0 U} \tau^{(x)} \quad \text{and} \quad \partial_z u_2 = \frac{D\gamma}{A_0 U} \tau^{(y)} \quad \text{on} \quad z = 0,$$

which lead to

$$u_3^b(t, x, y, \xi) = \frac{D\gamma \varepsilon \nu_V}{A_0 U} \left(\text{curl } \tau - \left(\cos \xi \text{curl } \tau + \sin \xi (\partial_x \tau^{(y)} + \partial_y \tau^{(x)}) \right) e^\xi \right),$$

where ξ is defined by $\xi = z/\sqrt{2\varepsilon \nu_V}$. Therefore, we obtain

$$(1.29) \quad u_3^1(t, x, y, 0) = -\lim_{\varepsilon \rightarrow -\infty} \frac{1}{\varepsilon} u_3^b(t, x, y, \xi) = -\beta \text{curl } \tau \quad \text{if} \quad \beta = \frac{\gamma}{\varepsilon \rho U^2},$$

which defines the relevant scale γ of the wind τ . Notice that there is no Ekman pumping in this case.

Remark. Summing (1.27) and (1.29), we get (0.1), (0.2), (0.3) with $Re = \nu_H^{-1}$.

Let us observe at this point that (0.1), (0.2), (0.3) can be reformulated as follows:

$$(1.30) \quad \operatorname{curl} \left(\partial_t u + u \cdot \nabla u - \frac{1}{Re} \Delta u + \frac{r_0}{2} u - (\eta_B + \beta y) u^\perp - \beta \tau \right) = 0,$$

$$(1.31) \quad u = (u_1, u_2), \quad u_1 = -\partial_y p, \quad u_2 = \partial_x p, \quad \text{and} \quad u|_{\partial\Omega} = 0.$$

Here, b^\perp denotes $(-b_2, b_1)$ for any $b = (b_1, b_2) \in \mathbb{R}^2$. Subsequently, (0.1), (0.2), (0.3) can formally be expressed as the two-dimensional incompressible Navier–Stokes equations

$$(1.32) \quad \partial_t u + u \cdot \nabla u - \frac{1}{Re} \Delta u + \frac{r_0}{2} u - (\eta_B + \beta y) u^\perp - \beta \tau + \nabla \pi = 0,$$

$$(1.33) \quad \operatorname{div} u = 0, \quad u|_{\partial\Omega} = 0.$$

Notice that (0.1), (0.2), (0.3) are equivalent to (1.32), (1.33) in the case when Ω is simply connected. Indeed, under this assumption on Ω , any curl-free vector field is the gradient of a scalar field on Ω . However, since this section is concerned about formal arguments, we consider (1.32), (1.33) as the limit system for general domains.

2. Justification of the derivation. To justify the limiting process, we first prove existence of a global strong solution for the limit system (which is very close to the two-dimensional Navier–Stokes equations). Then we construct approximate solutions (at first order explicitly) and make an energy estimate on the difference between true and approximate solutions.

2.1. Global weak solutions for the original system. Let us observe that system (1.1) with boundary conditions (1.2), (1.3) in Ω_3 and viscous stress tensor defined in spherical coordinates by (1.15) has global weak solutions $u \in L^\infty(0, T; L^2(\Omega)) \cap L^2(0, T; H_0^1(\Omega))$ for all $T > 0$. As a matter of fact, Leray’s existence theorem for the incompressible Navier–Stokes equations with Dirichlet boundary conditions can be slightly modified in the present case. First notice that it stems from (1.2), (1.3) that u is everywhere tangent to the boundary. The formal energy equality therefore reads as

$$(2.1) \quad \begin{aligned} \int_{\Omega_3} \rho |u(t, \cdot)|^2 + \int_0^t \int_{\Omega_3} (d : \sigma) ds &= \int_0^t \int_{\partial\Omega_3 \cap \{z=0\}} u(s, \cdot) \cdot \sigma \cdot e_r ds + \int_0^t \int_{\Omega_3} \rho g \cdot u ds \\ &= \gamma \int_0^t \int_{\partial\Omega_3 \cap \{z=0\}} \left(u_1(s, \cdot) \tau^{(x)} + u_2(s, \cdot) \tau^{(y)} \right) ds + \int_0^t \int_{\Omega_3} \rho g \cdot u ds. \end{aligned}$$

Observing that for $\alpha = \min \{A_H, A_V, 0\}$, we have

$$(2.2) \quad \int_0^t \int_{\Omega_3} (d : \sigma)(s, \cdot) ds \geq \alpha \int_0^t \int_{\Omega_3} |\nabla_{x,y,z} u|^2(s, \cdot) ds,$$

and that the trace theorem yields

$$\left| \int_0^t \int_{\partial\Omega_3 \cap \{z=0\}} \left(u_1 \tau^{(x)} + u_2 \tau^{(y)} \right) (s, \cdot) ds \right| \leq C \int_0^t |\tau|_{H^{-\frac{1}{2}}(\partial\Omega_3 \cap \{z=0\})} |u|_{H^1(\Omega_3)} ds,$$

we conclude by using classical compactness arguments. Notice that the assumption that A_0 is positive is essential to recover the classical H^1 bound on u . This is an ad hoc mathematical choice that is not justified from a physical viewpoint.

2.2. Strong solutions for the limit system. Let us turn to the proof of existence of global strong solutions for the limit system (1.32), (1.33). As previously mentioned, the wind-driven system has exactly the same features as the two-dimensional Navier–Stokes equations. We want here to prove the following theorem.

THEOREM 2.1. *Let $u_0 \in H_0^1(\Omega_2)$ such that $\operatorname{div} u_0 = 0$. Then there exists a global solution u of (1.32), (1.33) such that for all $T > 0$, $u \in L^\infty(0, T; H_0^1(\Omega_2))^2 \cap L^2(0, T; H^2(\Omega_2))^2$.*

Proof. First of all, standard compactness methods yield the existence of global weak solutions (u, p) of (1.32), (1.33) such that for all $T > 0$, $u \in L^\infty(0, T; L^2(\Omega_2)) \cap L^2(0, T; H_0^1(\Omega_2))$. In order to apply classical regularity theorems on the two-dimensional Navier–Stokes evolution problem, we write (1.32), (1.33) as follows:

$$(2.3) \quad \partial_t u + u \cdot \nabla u - \frac{1}{Re} \Delta u + \nabla p = f, \quad \operatorname{div} u = 0 \quad \text{and} \quad u|_{\partial\Omega} = 0,$$

where

$$(2.4) \quad f = (\eta_B + \beta y)u^\perp - \frac{r_0}{2}u + \beta\tau.$$

As a result, since f belongs to $L^2((0, T) \times \Omega_2)$, we deduce from [11] that assuming $u_0 \in H_0^1(\Omega_2)$ and $\operatorname{div} u_0 = 0$, then u is unique and for all $T > 0$

$$\partial_t u \quad \text{and} \quad \nabla p \in L^2((0, T) \times \Omega_2), \quad u \in L^\infty(0, T; H_0^1(\Omega_2)) \cap L^2(0, T; H^2(\Omega_2)).$$

2.3. Energy estimates.

THEOREM 2.2. *Let $\zeta^{ini} \in H^2(\Omega_2)$ and let us assume (1.17). There exist global weak solutions u^ε of (1.1) with initial data*

$$u_1^\varepsilon(0, \phi, \theta, r) = -\partial_y \zeta^{ini}(\phi r_* \cos \theta_0, (\theta - \theta_0)r_*),$$

$$u_2^\varepsilon(0, \phi, \theta, r) = \partial_x \zeta^{ini}(\phi r_* \cos \theta_0, (\theta - \theta_0)r_*), \quad \text{and} \quad u_3^\varepsilon(0, \phi, \theta, r) = 0$$

such that

$$(t, x, y, z) \mapsto u^\varepsilon \left(t, \frac{x}{r_* \cos \theta_0}, \theta_0 + \frac{y}{r_*}, r_0(1 + \delta z/r_*) \right)$$

converges strongly in $L^\infty(0, T; L_{loc}^2(\tilde{\Omega}_2^\varepsilon))$ to $(-\partial_y \zeta(t, x, y), \partial_x \zeta(t, x, y), 0)$ for all $T > 0$, where

$$\tilde{\Omega}_2^\varepsilon = \{(x, y, z) \mid (x, y) \in \Omega_2 \quad \text{and} \quad -1 + \varepsilon\eta_B \leq z \leq 0\}$$

and where $\zeta(t, x, y)$ is the solution of (1.7), (1.8), (1.9) with initial data $\zeta^0(x, y)$.

Notice that we assume that the initial data are “well prepared” in the sense that they satisfy the limit conditions (1.19). If they do not fit (1.19), waves of high speed propagate through the medium (see [7] for instance).

Sketch of the proof. As the energy estimates that follow have already been written in [7] and [10], we will not detail them completely.

The first step is to construct an approximate solution \tilde{u}^ε . For this we start from $u_1^0, u_2^0, u_3^0 = 0$ solutions of (1.7), (1.8), (1.9). Using (1.24), (1.25) at $z = 0$ and similar expressions at $z = 1$, we construct boundary layer profiles $u_1^b, u_2^b, u_3^b, u_1^t, u_2^t, u_3^t$. At this point, $u_1^0 + u_1^b + u_1^t, u_2^0 + u_2^b + u_2^t$ and $u_3^0 + u_3^b + u_3^t$ are divergence free but do

not match exactly the boundary conditions, since $u_1^0 + u_1^b + u_1^t$ is of order $\exp(-C/\varepsilon)$. It is straightforward, however, to add a divergence-free vector field that matches the boundary conditions.

The second step is to bound $v^\varepsilon = u^\varepsilon - \tilde{u}^\varepsilon$ by subtracting the equation on \tilde{u}^ε from the equation on u^ε , multiplying by v^ε , exactly as in [10]. As it can be deduced from the energy proof for the Munk layer (which is a more singular problem), no further details will be given here. \square

3. Sverdrup relation and Munk layer. The next step of the analysis of the homogeneous model of the wind-driven oceanic circulation is to study lateral boundary layers near shores. This is in fact one of the main interests of this very modeled system to explain an important geophysical feature, namely, the western intensification of boundary currents. For instance, in the northern Atlantic Ocean, a clockwise gyre possesses modest speeds of the order of 1 to 10 cm/s except in the intense and narrow Gulf Stream current along North America. The current velocity is typically 100 cm/s and has width of order 50 km. Similar phenomena occur in the Pacific Ocean (Kuroshio current), South Atlantic (Brazil current), and off East Africa (Agulhas current).

3.1. Formal limit.

3.1.1. Geometrical preliminaries. Let us begin the study of the limit

$$(3.1) \quad \beta \rightarrow +\infty, \quad r_0 \sim 1, \quad Re \sim 1, \quad \tau(t, x, y) \text{ given,}$$

of (1.7), (1.8), (1.9) in a smooth domain Ω_2 . In order to simplify the geometry, we will assume that Ω_2 is of the form

$$\Omega_2 = \{\chi_W(y) \leq x \leq \chi_E(y)\}$$

for $y_{\min} \leq y \leq y_{\max}$, with $\chi_W(y_{\min}) = \chi_E(y_{\min})$ and $\chi_W(y_{\max}) = \chi_E(y_{\max})$, where χ_W and χ_E are given functions of y , smooth on (y_{\min}, y_{\max}) . Next, the western and eastern boundaries Γ_W and Γ_E are defined by, respectively,

$$\Gamma_E = \{(\chi_E(y), y), y \in [y_{\min}, y_{\max}]\} \quad \text{and} \quad \Gamma_W = \{(\chi_W(y), y), y \in [y_{\min}, y_{\max}]\}.$$

We also define Ω_W and Ω_E by

$$\Omega_W = \{(x, y), \chi_W(y) \leq x < +\infty\} \quad \text{and} \quad \Omega_E = \{(x, y), -\infty < x \leq \chi_E(y)\}.$$

Let us introduce the small-scale $\varepsilon = (Re\beta)^{-1/3}$ and reduced variables z_l and z_r :

$$(3.2) \quad z_l = \frac{(x - \chi_W(y))D_W(y)}{\varepsilon} \quad \text{and} \quad z_r = \frac{(x - \chi_E(y))D_E(y)}{\varepsilon},$$

where D_W is defined by

$$D_W = (\cos \theta_W(y))^{4/3}, \quad \cos \theta_W = \frac{1}{\sqrt{1 + \chi_W'(y)^2}}, \quad \sin \theta_W = -\frac{\chi_W'(y)}{\sqrt{1 + \chi_W'(y)^2}},$$

and D_E has a similar expression, replacing θ_W and χ_W by θ_E and χ_E . Here, $\theta_W + \pi$ and θ_E denote respectively the angles with the unit vector e_x along the x variable of the outward normal on the west coast Γ_W and on the east coast Γ_E . The above expressions for z_l and z_r easily yield by differentiation

$$(3.3) \quad \partial_x z_l = \frac{D_W}{\varepsilon}, \quad \partial_y z_l = \frac{\tan \theta_W(y)}{\varepsilon} \left(D_W - \frac{4}{3} \varepsilon z_l \theta_W'(y) \right),$$

and similarly for z_r . Let Ψ be a function of $(x, y, z_l(x, y))$. We formally have at the leading order in ε

$$(3.4) \quad \Delta_{x,y} \Psi \sim \left(\frac{D_W}{\varepsilon} \right)^2 (1 + (\tan \theta_W)^2) \partial_{z_l}^2 \Psi \quad \text{and} \quad \Delta_{x,y}^2 \Psi \sim \frac{D_W}{\varepsilon^4} \partial_{z_l}^4 \Psi.$$

3.1.2. Sverdrup relation. At order β in the interior of the domain, we obtain the so-called Sverdrup relation

$$(3.5) \quad \partial_x p^0 = \text{curl } \tau.$$

Hence, we can choose p^0 such that $\nabla^\perp p^0$ is tangent to the boundary Γ_E :

$$(3.6) \quad p^0(t, x, y) = \int_{\chi_E(y)}^x \text{curl } \tau(t, x', y) dx'.$$

This choice is linked to the properties of the boundary layers. In fact Γ_E cannot bear a large layer (see next paragraph). Let us define a quantity that plays an important role in what follows:

$$(3.7) \quad \Phi(t, y) = \int_{\chi_E(y)}^{\chi_W(y)} \text{curl } \tau(t, x', y) dx'.$$

3.1.3. Boundary layers. Since $U^0 = \nabla^\perp p^0$ does not vanish on the boundary, we introduce a boundary layer correction p_b , which is given by the balance between the terms $\beta \partial_x p$ and $Re^{-1} \Delta^2 p$:

$$(3.8) \quad \begin{cases} -\Delta^2 p_b + \varepsilon^{-3} \partial_x p_b = 0 & \text{in } \Omega_2, \\ \nabla^\perp p_b = -U^0 & \text{on } \partial\Omega_2. \end{cases}$$

We will not solve (3.8) directly. Instead we look for an approximate solution of (3.8) of the form $p_l + p_r$, functions of (z_l, y) and (z_r, y) , p_l being the solution of an equation similar to (3.8) in Ω_W and p_r to a similar equation in Ω_E . More precisely let p_l and p_r be solutions of

$$(3.9) \quad \begin{cases} -\partial_{z_l}^4 p_l + \partial_{z_l} p_l = 0 & \text{in } \Omega_W, \\ \partial_{z_l} p_l|_{z_l=0} = -\varepsilon \frac{\text{curl } \tau(t, \chi_W(y), y)}{D_W(y)}, & p_l|_{z_l=0} = -\Phi(t, y), \\ p_l \rightarrow 0 & \text{when } z_l \rightarrow +\infty, \end{cases}$$

and

$$(3.10) \quad \begin{cases} -\partial_{z_r}^4 p_r + \partial_{z_r} p_r = 0, & \text{in } \Omega_E \\ \partial_{z_r} p_r|_{z_r=0} = -\varepsilon \frac{\text{curl } \tau(t, \chi_E(y), y)}{D_E(y)}, & p_r \rightarrow 0 \text{ when } z_r \rightarrow -\infty. \end{cases}$$

(We can impose only one condition at $z_r = 0$ on (3.10).) We have

$$(3.11) \quad \begin{aligned} p_l = & -\Phi(t, y) \left(\cos \left(\frac{\sqrt{3}}{2} z_l \right) + \frac{1}{\sqrt{3}} \sin \left(\frac{\sqrt{3}}{2} z_l \right) \right) e^{-z_l/2} \\ & - 2\varepsilon \frac{\text{curl } \tau(t, \chi_W(y), y)}{\sqrt{3} D_W(y)} \sin \left(\frac{\sqrt{3}}{2} z_l \right) e^{-z_l/2}, \end{aligned}$$

$$(3.12) \quad p_r = -\varepsilon \frac{\text{curl } \tau(t, \chi_E(y), y)}{D_E(y)} e^{z_r}.$$

Let us introduce \mathcal{P}_l and \mathcal{P}_r defined by

$$\mathcal{P}_l = \left\{ \left(P(z_l) \cos \left(\frac{\sqrt{3}}{2} z_l \right) + Q(z_l) \sin \left(\frac{\sqrt{3}}{2} z_l \right) \right) e^{-kz_l/2}, (P, Q) \in \mathcal{A}^2, k \in \mathbb{N}^* \right\},$$

$$\mathcal{P}_r = \{ P(z_r) e^{kz_r}, P \in \mathcal{A}, k \in \mathbb{N}^* \},$$

where \mathcal{A} denotes the space of polynomials in z with suitably smooth coefficients in $y \in [y_{\min}, y_{\max}]$. Considering p_l and p_r as functions of x and y , we obtain

$$(3.13) \quad \begin{cases} -\Delta^2 p_l + \frac{1}{\varepsilon^3} \partial_x p_l = \frac{1}{\varepsilon^3} R_l^0, \\ \partial_x p_l = -\text{curl } \tau(t, \chi_W(y), y), \end{cases} \quad p_l = -\Phi(t, y) \quad \text{on } \Gamma_W,$$

and

$$(3.14) \quad \begin{cases} -\Delta^2 p_r + \frac{1}{\varepsilon^3} \partial_x p_r = \frac{1}{\varepsilon^3} R_r^1, \\ \partial_x p_r = -\text{curl } \tau(t, \chi_E(y), y), \end{cases} \quad p_r = -\varepsilon \frac{\text{curl } \tau(t, \chi_E(y), y)}{D_E(y)} \quad \text{on } \Gamma_E,$$

where $R_l^0 \in \mathcal{P}_l$ and $R_r^1 \in \mathcal{P}_r$.

Remarks.

- By construction, on Γ_W

$$(3.15) \quad \partial_x(p^0 + p_l) = 0, \quad p^0 + p_l = 0,$$

and on Γ_E

$$(3.16) \quad \partial_x(p^0 + p_r) = 0, \quad p^0 + p_r = -\varepsilon \frac{\text{curl } \tau(t, \chi_E(y), y)}{D_E(y)}.$$

- Notice that in the boundary layer, the leading term of u_2 is proportional to

$$\varepsilon^{-1} \Phi(t, y) D_W(y) \sin \left(\frac{\sqrt{3}}{2} z_l \right) e^{-z_l/2}.$$

Hence it is of order $\varepsilon^{-1} D_W(y)$ and very large in a band of typical size $(\varepsilon D_W(y))^{-1}$. The above boundary layers are called Munk layers [15]. Notice that they degenerate when $\cos(\theta_W(y)) = 0$, which corresponds to northern or southern boundaries. We refer to [15] for a thorough discussion and comparison with measurements and numerical experiments.

- In order to avoid steep singularities when approaching the extremal points $N = (\chi_E(y_{\max}), y_{\max})$ and $S = (\chi_E(y_{\min}), y_{\min})$, we will assume that the irrotational part of the wind vanishes in a neighborhood of N and S . More precisely, we suppose that there exists $\lambda > 0$ such that $\text{curl } \tau \equiv 0$ when $y \in [y_{\max} - \lambda, y_{\max}] \cup [y_{\min}, y_{\min} + \lambda]$.

3.1.4. Construction of an approximate solution.

PROPOSITION 3.1. *Let $\tau(t, x, y) \in L^\infty((0, T); H^s)$ be given and N be an integer. If s is large enough, there exists on $[0, T]$ an approximate solution p^{app} of the form*

$$p^{app}(t, x, y) = \sum_{i=0}^N \varepsilon^i p_{int}^i(t, x, y) + \sum_{i=0}^N \varepsilon^i p_W^i(t, x, z_W) + \sum_{i=0}^N \varepsilon^i p_E^i(t, x, z_E) + \varepsilon^N \tilde{p}^N,$$

where p_W^i and p_E^i are smooth functions, rapidly decreasing in z_W and z_E , p_{int} is smooth, such that with $u^{app} = \nabla^\perp p^{app}$,

$$\begin{aligned} \partial_t u^{app} + (u^{app} \cdot \nabla) u^{app} + \frac{r_0}{2} u^{app} - Re^{-1} \Delta u^{app} - (\eta_B + \beta y) u^{app\perp} + \nabla \pi \\ = \beta \operatorname{curl} \tau + \nabla^\perp R_1 + R_2 \end{aligned} \quad (3.17)$$

with

$$u_{|\partial\Omega_2}^{app} = 0, \quad \operatorname{div} u^{app} = 0, \quad (3.18)$$

and

$$|R_2|_{L^\infty(0,T;L^2(\Omega_2))} + |R_1|_{L^\infty(0,T;L^2(\Omega_2))} \leq C\sqrt{\varepsilon}^{N-1} \quad (3.19)$$

for some constant $C > 0$ independent of ε . Moreover, $u^{app} = u_{int} + u_W + u_E$, where ∇u_{int} is bounded in $L^\infty((0,T) \times \Omega_2)$ and

$$\begin{aligned} |\nabla u_W(t, x, y)| \leq C_\lambda \left(\left(\frac{1}{\varepsilon^2} |\Phi(t, \cdot)|_{L^\infty(y_{\min}, y_{\max})} + \frac{1}{\varepsilon} |\operatorname{curl} \tau(t, \cdot)|_{H^s(\Omega_2)} \right) \right. \\ \left. \times Q_l(z_l) e^{-Cz_l} + |\operatorname{curl} \tau(t, \cdot)|_{H^s(\Omega_2)} \right) 1_{y_{\min} + \lambda \leq y \leq y_{\max} - \lambda}, \end{aligned} \quad (3.20)$$

$$|\nabla u_E(t, x, y)| \leq C_\lambda |\operatorname{curl} \tau(t, \cdot)|_{H^s(\Omega_2)} \left(\frac{1}{\varepsilon} Q_r(z_r) e^{Cz_r} + 1 \right) 1_{y_{\min} + \lambda \leq y \leq y_{\max} - \lambda}, \quad (3.21)$$

where Q_l and Q_r are some polynomials with constant coefficients.

Sketch of the proof. p_{int}^0 , p_W^0 , and p_E^0 were calculated in the previous section. The other profiles p_{int}^i , p_W^i , and p_E^i can be obtained by solving similar equations, taking into account the error terms created by the lower-order profiles. \tilde{p}^N is then an arbitrary smooth bounded function such that $\nabla p^{app} = 0$ on Γ_W and Γ_E . As the construction is straightforward but tedious, we will not detail it here and we refer in particular to [9, 3] for complete constructions in similar cases. \square

3.2. Justification of the asymptotics $\beta \rightarrow +\infty$. Notice that in the boundary layer the northward velocity is of order ε^{-1} , and hence very large. Its gradient is even larger and of size ε^{-2} . The behavior in the layer is therefore very singular (much more singular than in Ekman-type boundary layers for instance). In order to control this large term by the viscosity, we will in fact need to keep Re small enough. This limitation is linked to the physically expected behavior: recirculation problems occur near northern boundaries, which appear to be unstable when Re becomes large (see [16] for the derivation of inertial boundary layers and some numerical simulations). Moreover, in order to avoid problems near northern and southern boundaries (that is, near y_{\max} or y_{\min}), we are led to assume that $\operatorname{curl} \tau$ vanishes for $y_{\max} - \lambda \leq y \leq y_{\max}$ and $y_{\min} \leq y \leq y_{\min} + \lambda$ for some $\lambda > 0$ (the size of the boundary layer grows as y approaches y_{\min} or y_{\max}), which means we don't have to make a technical study of the layer near y_{\min} and y_{\max} . More precisely, we have the following theorem.

THEOREM 3.2. *Let $\delta > 0$. Let τ be such that $\operatorname{curl} \tau \in L^\infty((0,T); H^s(\Omega_2))$ ($s \geq 2$) for some $T > 0$, let u^{app} be given by Proposition 3.1 with $N \geq 2$, and let u_ε^{ini} be such that $u_\varepsilon^{ini} \cdot n = 0$ on $\partial\Omega_2$ and $u_\varepsilon^{ini} - u_{|t=0}^{app} \rightarrow 0$ in $L^2(\Omega_2)$. Assume that there exists $\lambda > 0$ such that*

$$\operatorname{curl} \tau \equiv 0 \quad \text{for} \quad y_{\min} \leq y \leq y_{\min} + \lambda \quad \text{or} \quad y_{\max} - \lambda \leq y \leq y_{\max}. \quad (3.22)$$

Denoting by u_ε the solution of (0.1, 0.2, 0.3) with initial data u_ε^{ini} , there exists $C_0 > 0$ depending only on λ such that if

$$(3.23) \quad \left| \int_{\chi_W(y)}^{\chi_E(y)} \text{curl} \tau(t, x', y) dx' \right|_{L^\infty((0, T) \times (y_{\min}, y_{\max}))} < C_0 Re^{-1},$$

then

$$(3.24) \quad u_\varepsilon - u^{app} \rightarrow 0 \quad \text{in} \quad L^\infty((0, T); L^2(\Omega_2)).$$

Let us emphasize that the theorem holds only for small enough wind, this limitation being a physical one.

Proof. Let us define \bar{U} by $\bar{U} = u_\varepsilon - u^{app}$. Notice that \bar{U} satisfies for some pressure \bar{p}

$$(3.25) \quad \partial_t \bar{U} + (u_\varepsilon \cdot \nabla) \bar{U} + (\bar{U} \cdot \nabla) u^{app} + \frac{r_0}{2} \bar{U} - (\eta_B + \beta y) \bar{U}^\perp - \frac{1}{Re} \Delta \bar{U} + \nabla \bar{p} = \nabla^\perp R_1 + R_2$$

and

$$(3.26) \quad \text{div } \bar{U} = 0, \quad \bar{U}|_{t=0} = 0 \quad \text{and} \quad \bar{U}|_{\partial\Omega_2} = 0.$$

Multiplying (3.25) by \bar{U} and integrating over Ω_2 , we obtain

$$(3.27) \quad \begin{aligned} & \frac{1}{2} \int_{\Omega_2} |\bar{U}|^2(t, x) dx + \frac{r_0}{2} \int_0^t \int_{\Omega_2} |\bar{U}|^2 dx ds + Re^{-1} \int_0^t \int_{\Omega_2} |\nabla \bar{U}|^2 dx ds \\ & \leq \left| \int_0^t \int_{\Omega_2} \bar{U} \cdot [(\bar{U} \cdot \nabla) u^{app}] dx ds \right| + \int_0^t \int_{\Omega_2} (|\nabla \bar{U}| |R_1| + |\bar{U}| |R_2|) dx ds. \end{aligned}$$

As ∇u_{int} is bounded, we have only to take care of $\nabla u_W + \nabla u_E$. For this we write in the neighborhood of the west coast

$$\begin{aligned} |\bar{U}(t, x, y)| & \leq C(x - \chi_W(y))^{1/2} \left(\int_{\chi_W(y)}^x |\partial_x \bar{U}|^2 dx' \right)^{1/2} \\ & \leq C \left(\frac{z_l \varepsilon}{D_W} \right)^{1/2} \left(\int_{\chi_W(y)}^{\chi_E(y)} |\partial_x \bar{U}|^2 dx' \right)^{1/2}. \end{aligned}$$

Similarly, we have near the east coast

$$(3.28) \quad |\bar{U}(t, x, y)| \leq C \left(\frac{|z_r| \varepsilon}{D_E} \right)^{1/2} \left(\int_{\chi_W(y)}^{\chi_E(y)} |\partial_x \bar{U}|^2 dx' \right)^{1/2}.$$

Hence, we deduce from (3.20) that

$$(3.29) \quad \begin{aligned} \int_{\Omega_2} |\nabla u_W| |\bar{U}|^2 dx dy & \leq C_\lambda |\text{curl } \tau|_{H^s} \int_{\Omega_2} |\bar{U}|^2 dx dy + C_\lambda \int_{\Omega_2} \left(\left(\int_{\chi_W(y)}^{\chi_E(y)} |\partial_x \bar{U}|^2 dx' \right) \right. \\ & \quad \left. \times z_l Q_l(z_l) e^{-C z_l} \left(\frac{1}{\varepsilon} |\Phi|_{L^\infty} + |\text{curl } \tau|_{H^s} \right) 1_{y_{\min} + \lambda \leq y \leq y_{\max} - \lambda} \right) dx dy. \end{aligned}$$

Using the fact that $dx dy = \varepsilon D_W^{-1} dz_l dy$, we obtain

$$(3.30) \quad \begin{aligned} \int_{\Omega_2} |\nabla u_W| |\bar{U}|^2 dx dy &\leq C_{T,\lambda} \int_{\Omega_2} |\bar{U}|^2 dx dy \\ &+ C_\lambda |\nabla \bar{U}|_{L^2(\Omega_2)}^2 (|\Phi|_{L^\infty} + \varepsilon |\operatorname{curl} \tau|_{H^s}) \int_0^{+\infty} z Q_l(z) e^{-Cz} dz. \end{aligned}$$

The same estimates yield for the other term

$$(3.31) \quad \begin{aligned} \int_{\Omega_2} |\nabla u_E| |\bar{U}|^2 dx dy &\leq C_{T,\lambda} \int_{\Omega_2} |\bar{U}|^2 dx dy \\ &+ \varepsilon C_\lambda |\nabla \bar{U}|_{L^2(\Omega_2)}^2 |\operatorname{curl} \tau|_{H^s} \int_0^{+\infty} z Q_l(z) e^{-Cz} dz. \end{aligned}$$

Inserting (3.30), (3.31) in (3.27), we obtain

$$(3.32) \quad \begin{aligned} \int_{\Omega_2} |\bar{U}|^2(t, x) dx + Re^{-1} \int_0^t \int_{\Omega_2} |\nabla \bar{U}|^2 dx ds &\leq C_T \varepsilon^{\frac{N-1}{2}} + C_{T,\lambda} \int_0^t \int_{\Omega_2} |\bar{U}|^2 dx ds \\ &+ (C_\lambda |\phi|_{L^\infty((0,T) \times (y_{\min}, y_{\max}))} + \varepsilon C_{T,\lambda}) \int_0^t \int_{\Omega_2} |\nabla \bar{U}|^2 dx ds. \end{aligned}$$

The last term of the right-hand side can be absorbed in the viscosity term provided the strength measured by $|\Phi|_{L^\infty((0,T) \times (y_{\min}, y_{\max}))}$ is small enough compared to Re^{-1} . \square

4. Stommel layer. In this section, we focus on the case when the effect of the bottom Ekman layer cannot be neglected. Let us define ε_s as follows:

$$(4.1) \quad \varepsilon_s = \frac{r_0}{2\beta}.$$

Even though r_0 was taken to be constant in the previous section, the case when $\varepsilon/\varepsilon_s \rightarrow +\infty$ can be treated similarly since bottom friction is negligible everywhere. When $\varepsilon/\varepsilon_s \rightarrow 0$, we obtain two boundary layers, namely the Stommel layer and a frictional sublayer that we want to describe in this section. Again the viscosity will remain constant and does not go to zero, whereas the velocities will increase and are not bounded as ε_s goes to 0.

First of all, the Stommel layer stems from the balance between the Ekman pumping $\frac{r_0}{2} \Delta p$ and $\beta \partial_x p$:

$$(4.2) \quad \varepsilon_s \Delta p^s + \partial_x p^s = 0.$$

Let us introduce auxiliary variables z_l^s and z_r^s :

$$(4.3) \quad z_l^s = \frac{(x - \chi_W(y)) \cos^2 \theta_W(y)}{\varepsilon_s} \quad \text{and} \quad z_r^s = \frac{(x - \chi_E(y)) \cos^2 \theta_E(y)}{\varepsilon_s}.$$

Hence, considering p_l^s and p_r^s as functions of (x, y, z_l^s) and (x, y, z_r^s) , we obtain the following equation at the leading order in ε_s :

$$(4.4) \quad \partial_{z_l^s}^2 p^s + \partial_{z_r^s}^2 p^s = 0.$$

General solutions are expressed as follows:

$$(4.5) \quad p^s = C_1(t, x, y)e^{-z^s} + C_2(t, x, y).$$

Since we require that $p_l^s \rightarrow 0$ when $z_l^s \rightarrow +\infty$ and $p_r^s \rightarrow 0$ when $z_r^s \rightarrow -\infty$, we obtain $p_r^s \equiv 0$ and

$$(4.6) \quad p_l^s = -\Phi(t, y)e^{-z_l^s},$$

so that $\nabla^\perp(p^0 + p_l^s)$ is tangent to the boundary $\partial\Omega_2$ at the leading order in ε_s . In order to enforce the no-slip boundary condition for the velocity, we introduce a frictional sublayer on both sides of the boundary. This sublayer corresponds to the balance between $Re^{-1}\Delta^2 p$ and $r_0\Delta p/2$:

$$(4.7) \quad \varepsilon^3\Delta^2 p + \varepsilon_s\Delta p = 0.$$

Let z_l^f and z_r^f be the auxiliary variables defined by

$$(4.8) \quad z_l^f = \frac{(x - \chi_W(y)) \cos \theta_W(y)}{\varepsilon_f} \quad \text{and} \quad z_r^f = \frac{(x - \chi_E(y)) \cos \theta_E(y)}{\varepsilon_f},$$

where

$$(4.9) \quad \varepsilon_f = \varepsilon_s \left(\frac{\varepsilon}{\varepsilon_s} \right)^{3/2} \ll \varepsilon_s.$$

As before, we obtain an ordinary differential equation in z^f :

$$(4.10) \quad -\partial_{z^f}^4 p^f + \partial_{z^f}^2 p^f = 0.$$

In view of the conditions at infinity, we can write

$$(4.11) \quad p_l^f = C_3(t, x, y)e^{-z_l^f} \quad \text{and} \quad p_r^f = C_4(t, x, y)e^{z_r^f}.$$

Finally, in order to determine C_3 and C_4 , we require that $\partial_x(p^0 + p^f + p^s)$ vanishes on the boundary, so that

$$(4.12) \quad C_3(y) = \frac{\varepsilon_f}{\cos \theta_W(y)} \text{curl } \tau(t, \chi_W(y), y) + \frac{\varepsilon_f}{\varepsilon_s} \Phi(t, y) \cos \theta_W(y)$$

and

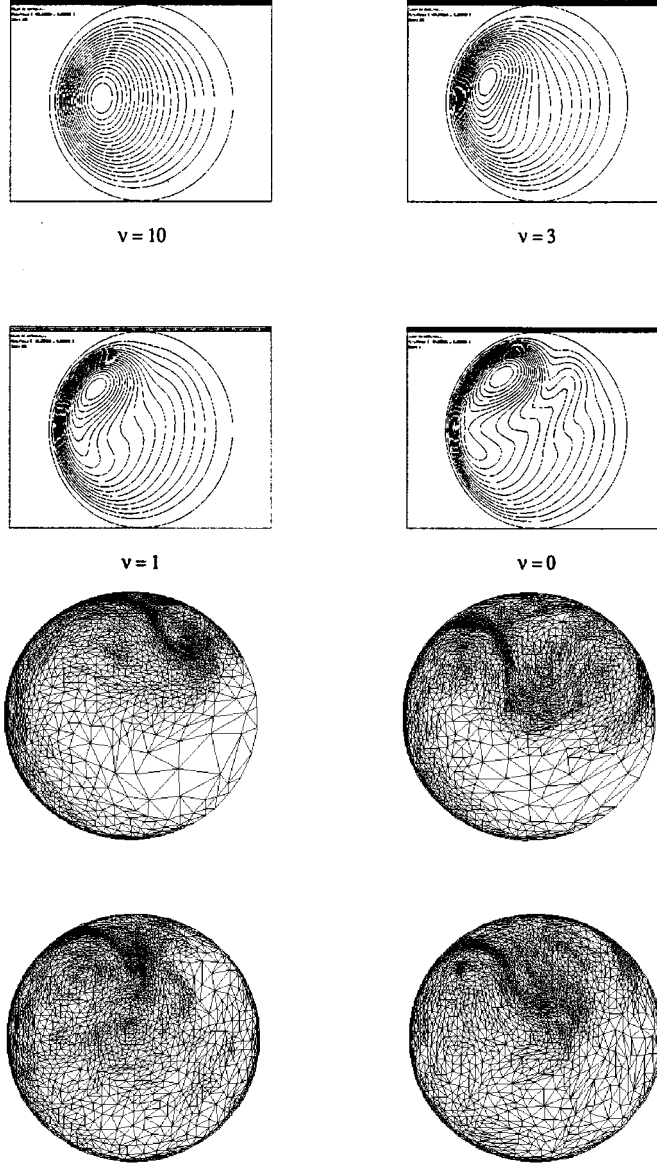
$$(4.13) \quad C_4(y) = -\frac{\varepsilon_f}{\cos \theta_E(y)} \text{curl } \tau(t, \chi_E(y), y).$$

Hence, the correction term reads on the west coast as

$$p_l^f = -\Phi(t, y)e^{-z_l^s} + \left(\frac{\varepsilon}{\varepsilon_s} \right)^{3/2} \left(\frac{\text{curl } \tau(t, \chi_W(y), y)}{\cos \theta_W(y)} + \Phi(t, y) \cos \theta_W(y) \right) e^{-z_l^f}$$

and on the east coast as

$$p_r^f = -\left(\frac{\varepsilon}{\varepsilon_s} \right)^{3/2} \frac{1}{\cos \theta_E(y)} \text{curl } \tau(t, \chi_E(y), y) e^{z_r^f}.$$

FIG. 5. *Time evolution with mesh adaption.*

As a result, the above construction yields a boundary layer term $\nabla^\perp p_b$ with a singularity in ε_s^{-1} multiplied by fast-decreasing exponentials, just as in the analysis of the Munk layer. Let us remark that the boundary layer velocity profile in the northern direction along the west coast remains positive, so that we do not have countercurrents like in the Munk layer. Assuming as in the previous section that the curl of the wind vanishes near N and S and that there exists $k \in \mathbb{N}^*$ such that $\varepsilon_s^k \leq \varepsilon \ll \varepsilon_s$ when passing to the limit $(\varepsilon_S, \varepsilon) \rightarrow 0$, it turns out that the same energy method applies for small enough winds without major modifications so that we do not get into further details of the proof.

5. Numerical simulations. This part is devoted to illustrations and numerical experiments on intensification of boundary currents in a circular ocean basin. All the simulations have been performed using the freefem package developed by Pironneau and coauthors.

Simulations clearly show a boundary layer-type behavior on the stream function near the left boundary. (We recall that the velocity, linked to the gradient of the stream function, is very large in this region.) The solution is not symmetric since the velocity is directed northward in the boundary, and therefore the “eye” is pushed toward the northwest direction. The size of the boundary layer is clearly limited by the numerical viscosity (see Figure 5)

Moreover, the equilibrium state strongly depends on the viscosity, and in particular on the numerical diffusion. In order to lower the viscosity of the scheme, we tried to use mesh adaptivity (see Figure 5) in the limit case $\nu = 0$ (small ν leads to similar results). It turns out that the results strongly depend on times when mesh adaptation is fulfilled. In addition, the flow tends to leave the boundary on the northwest side. This phenomenon can be explained as follows: first numerical viscosity stabilizes the flow. Then after adaptation, the mesh size becomes very small in the boundary layer. The local numerical viscosity is then small in the Munk layer. But this layer is known to be unstable at high Reynolds numbers. Hence an instability is created, which propagates in the whole domain: the stream function changes rapidly. New waves are created, which are damped by the viscosity. The second mesh adaptation leads to a completely different mesh, which again creates instabilities elsewhere.

Acknowledgments. The authors would like to thank Y. Brenier, P. Delecluse, and F. Dubois for many interesting discussions. The numerical simulations have been fulfilled using the freefem package of O. Pironneau and coauthors.

REFERENCES

- [1] T. COLIN, *Remarks on a homogeneous model of ocean circulation*, Asymptot. Anal., 12 (1996), pp. 153–168.
- [2] T. COLIN AND P. FABRIE, *Equations de Navier–Stokes 3D avec force de Coriolis et viscosité verticale évanescence*, C. R. Acad. Sci. Paris, Sér. I Math., 324 (1997), pp. 275–280.
- [3] B. DESJARDINS AND E. GRENIER, *Derivation of the quasigeostrophic potential equations*, Adv. Differential Equations, to appear.
- [4] V. W. EKMAN, *On the influence of the earth’s rotation on ocean currents.*, Ar. Mat. Astr. Fysik, Stockholm, 2 (11) (1905).
- [5] A. E. GILL, *Atmosphere Ocean Dynamics*, Academic Press, New York, 1982.
- [6] H. P. GREENSPAN, *The Theory of Rotating Fluids*, Cambridge Monogr. Mech. Appl. Math., Cambridge Univ. Press, Cambridge, New York, 1980.
- [7] E. GRENIER, *Oscillatory perturbations of the Navier–Stokes equations*, J. Math. Pures Appl., 76 (1997), pp. 477–498.
- [8] E. GRENIER, *Fluides tournants et ondes d’inertie*, C. R. Acad. Sci. Paris, 321 (1995), pp. 711–714.
- [9] E. GRENIER AND O. GUÉS, *Boundary layers for viscous perturbations of noncharacteristic quasilinear hyperbolic problems*, J. Differential Equations, 143 (1) (1998), pp. 110–146.
- [10] E. GRENIER AND N. MASMOUDI, *Ekman layers of rotating fluids, the case of well prepared data*, Comm. Partial Differential Equations, 22 (1997), pp. 953–975.
- [11] J. LERAY, *Essai sur les mouvements plans d’un liquide visqueux que limitent des parois*, J. Math. Pures Appl., 13 (1934), pp. 331–418.
- [12] R. LEWANDOWSKI, *Analyse mathématique et océanographique*, Recherches en Mathématiques Appliquées, Masson, Paris, Milan, Barcelona, 1997.
- [13] D. LEVERMORE, M. OLIVER, AND E. TITI, *Global well-posedness for models of shallow water in a basin with a varying bottom*, Indiana Univ. Math. J., 45 (1996), pp. 479–510.
- [14] J.-L. LIONS, R. TEMAM, AND S. WANG, *Modèles et analyse mathématiques du système océan/atmosphère*, C. R. Acad. Sci. Paris Sér. I Math., 316 (1993), pp. 113–119, C. R. Acad.

- Sci. Paris Sér. I Math., 316 (1993), pp. 211–215, C. R. Acad. Sci. Paris Sér. I Math., 318 (1994), pp. 1165–1171.
- [15] W. H. MUNK AND G. F. CARRIER, *The wind-driven circulation in ocean basins of various shapes*, Tellus, 2 (1950), pp. 158–167.
- [16] J. PEDLOSKY, *Geophysical Fluid Dynamics*, Springer-Verlag, Berlin, 1979.

Reproduced with permission of the copyright owner. Further reproduction prohibited without permission.